7th ECCOMAS Thematic Conference on Smart Structures and Materials
SMART 2015
A.L. Araújo, C.A. Mota Soares, et al. (Editors)

A HYBRID TRAILING EDGE CONTROL SURFACE CAPABLE OF CAMBER AND DECAMBER MORPHING

İlhan Ozan Tunçöz[*], Yosheph Yang[*], Ercan Gürses[*], Melin Şahin[*], Serkan Özgen[*], Yavuz Yaman[*]

[*]Middle East Technical University,
Department of Aerospace Engineering, Turkey
ozan.tuncoz@metu.edu.tr, yosheph.yang@metu.edu.tr, gurses@metu.edu.tr, msahin@metu.edu.tr, serkan.ozgen@ae.metu.edu.tr, yyaman@metu.edu.tr

Key words: Morphing Control Surface, Finite Element Analysis, Computational Fluid Dynamics, Aerodynamic Analysis, Structural Design

Summary: *This study presents the design and analysis of a novel hybrid trailing edge control surface that is capable to perform both camber and decamber morphing. The design was conducted with CATIA V5-6R2012 package program. Structural analyses were performed with Finite Element Method by using ANSYS® Workbench™ v14.0 package program both in in-vacuo condition and under aerodynamic loading. The aerodynamic loads were calculated by Computational Fluid Dynamics analyses. The required aerodynamic mesh was generated by Pointwise® V17.2 R2 package program, and SU2 (Stanford University Unstructured) V3.2.1 open source software was used as flow solver. The results prove that the designed control surface is capable of performing both camber and decamber morphing both in in-vacuo condition and under aerodynamic loading.*

1 INTRODUCTION

In the design of the conventional aerial vehicles, the aerodynamic performance at a certain flight regime is maximized with a unique shape of the wing. However, the requirements of the different flight conditions are generally conflicting throughout the entire flight. Therefore, the shape of the wing of the conventional aerial vehicles is designed such that the aerodynamic performance is maximized for the flight regime at which the aerial vehicle spends most of its mission time [1]. In off-design conditions, the aerial vehicles require additional mechanism such as flaps to eliminate the deficiency of the wing configuration. But it is known that the existing gaps between the wing and the flaps cause to decreased aerodynamic efficiency and increased aerodynamic noise [2]. Additionally, the fuel consumption of the aerial vehicles increase due to performance deficiencies and ultimately results in greater emissions of harmful CO_2 and NO_x gases to the environment.

In order to alleviate these adverse effects, the authors proposed a novel hybrid trailing edge control surface capable of performing camber and decamber morphing [3, 4]. The trailing edge control surface is designed in an unconventional manner, that is, there is no hinge and seam, and hence existing gaps are eliminated. The study is conducted within the scope of CHANGE (**C**ombined morp**H**ing **A**ssessment software usi**NG** flight **E**nvelope data

and mission based morphing prototype wing development) Project [5], which is a project of 7th Framework Programme of the European Commission.

2 THE DESIGN OF THE TRAILING EDGE CONTROL SURFACE

The design process of the trailing edge control surface was conducted by using CATIA V5-6R2012 package program. The designed control surface is a part of a baseline wing having NACA6510 airfoil. The control surface has a chord length of 180 [mm] and a span length of 900 [mm], and there is no pre-twist along the span of the control surface. The isometric view of the baseline wing and the trailing edge control surface is illustrated in Figure 1.

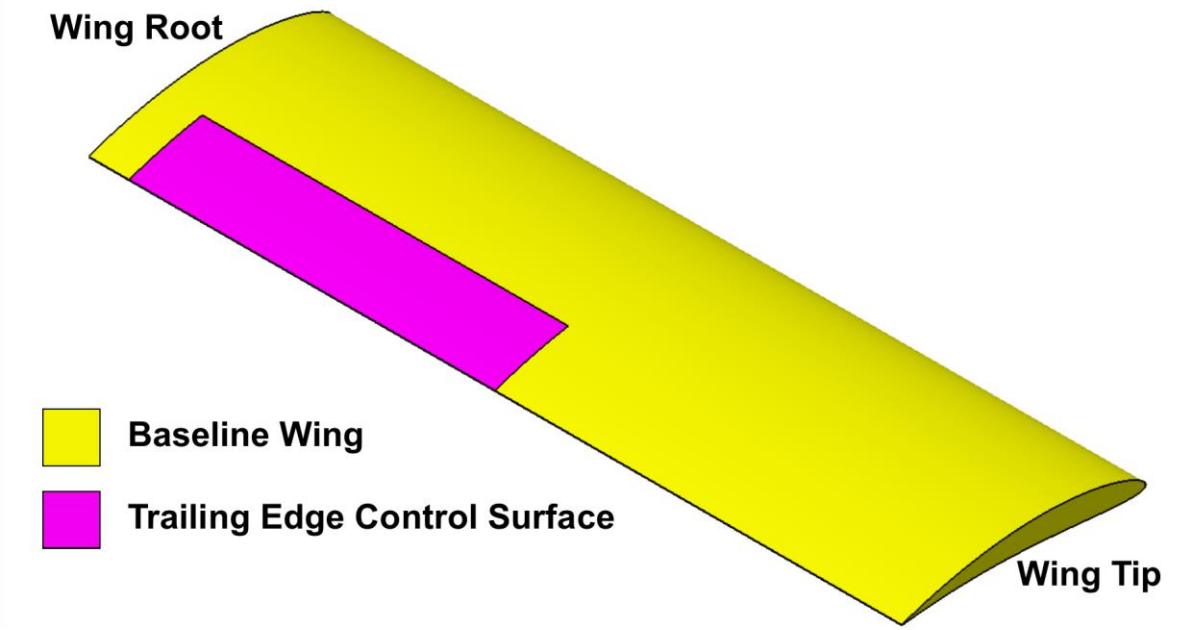

Figure 1: The Isometric View of the Baseline Wing and the Trailing Edge Control Surface

The main aim of the designed control surface is to perform specific camber and decamber morphing. In this context, NACA 8510 was selected to be the target profile for camber, while NACA 3510 and NACA 2510 were selected to be the target profiles for decamber. The target profiles are shown in Figure 2 along with the baseline profile, NACA 6510.

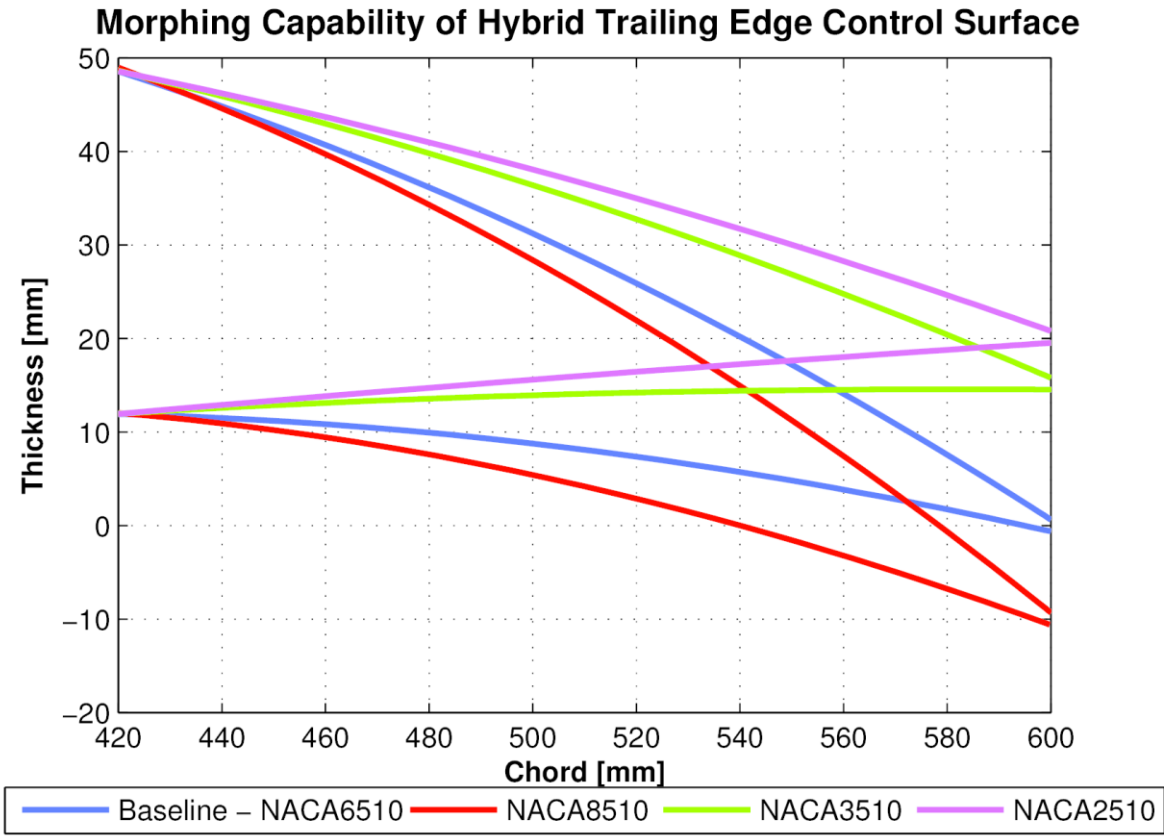

Figure 2: The Required Morphing Capabilities of the Hybrid Trailing Edge Control Surface

The designed trailing edge control surface is composed of three different materials, and hence named as hybrid trailing edge control surface. The main parts of the control surface are so-called the “C Part”, “Compliant Part”, “Rigid Part” and “Foam Part”. The side view of the hybrid trailing edge control surface is illustrated in Figure 3.

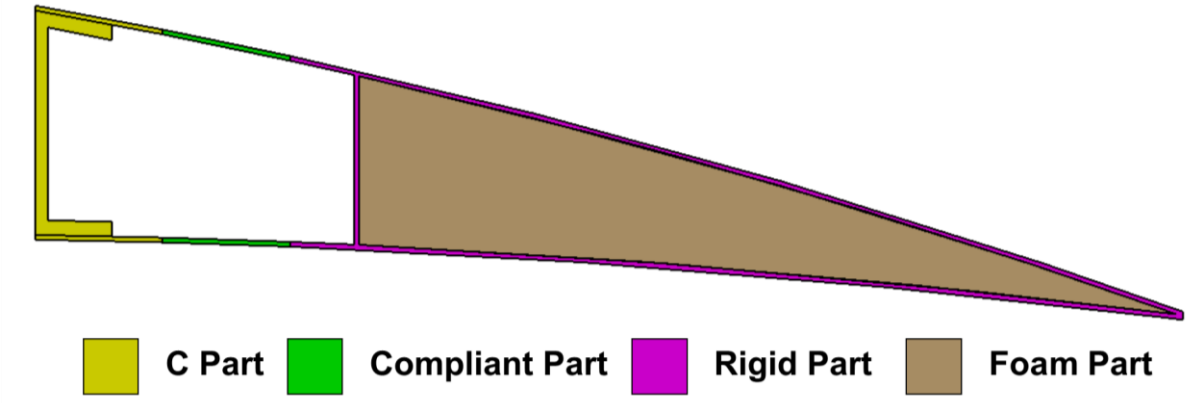

Figure 3: The Side View of the Hybrid Trailing Edge Control Surface

2.1 The Parts of the Control Surface

The primary purpose of C part is to connect the control surface to the wing. The lower and upper skin-like sections of the C part are made of glass-fibre prepreg EHG250-68-37 composite, and the C part itself is made of aluminum. The material properties of composite and aluminum are given in Table 1 and Table 2, respectively.

Density, ρ:	1900 [kg/m^3]
Young's Modulus, E_{11}:	24.5 [GPa]
Young's Modulus, E_{22}:	23.8 [GPa]
Poisson's Ratio, ν_{12}:	0.11
Shear Modulus, G_{12}:	4.7 [GPa]
Shear Modulus, G_{13}:	3.6 [GPa]
Shear Modulus, G_{23}:	2.6 [GPa]
Ply Thickness:	0.25 [mm]

Table 1: The Material Properties of Glass-Fibre Prepreg EHG250-68-37 Composite [6]

Density, ρ:	2770 [kg/m^3]
Young's Modulus, E:	71 [GPa]
Poisson's Ratio, ν:	0.33

Table 2: The Material Properties of Aluminum [7]

The compliant part of the control surface is made of a silicone based material [8]. In order to determine the material properties of the silicone, a uniaxial test was conducted. The resultant stress-strain curve is presented in Figure 4. The density of silicone was assigned to 1250 [kg/m^3] [9].

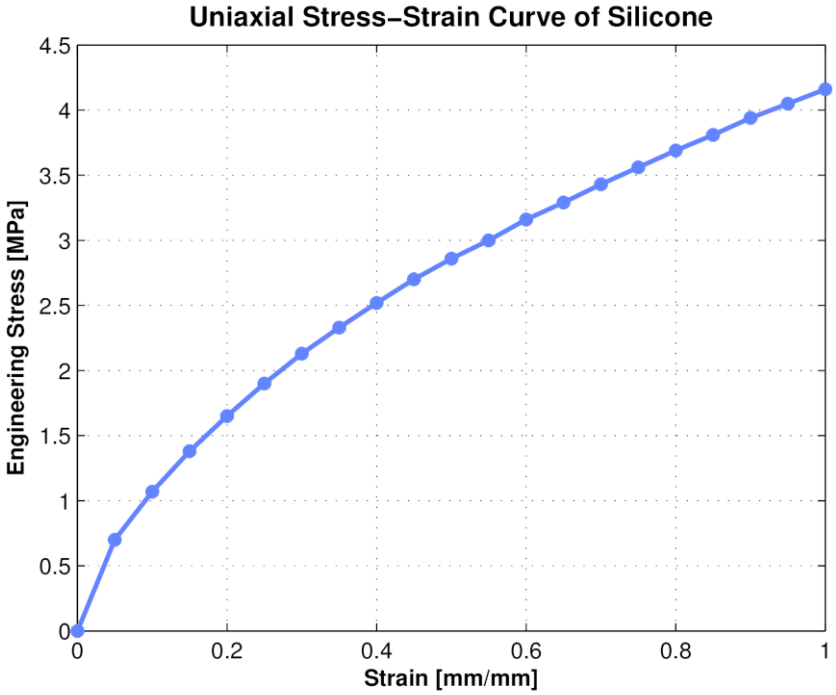

Figure 4: Uniaxial Stress-Strain Curve of Silicone

The compliant part is always intended to have tension both in upper and lower parts during the deflection of the control surface. This is necessary in order to avoid any possible slack in the compliant part which could occur when the part is subjected to compression. The differential extension of the compliant parts results in deflection of the control surface. In order to camber the control surface, the upper compliant part should be extended more than its lower counterpart, and vice versa for decamber.

The rigid part is made of glass-fibre prepreg EHG250-68-37 composite and the volume of that part, called as foam part, is filled with Rohacell® 51 RIMA foam material in order to increase the transverse stiffness of the control surface under the aerodynamic loading. The material properties of the Rohacell® 51 RIMA foam material is given is Table 3.

Density, ρ:	52 [kg/m^3]
Young's Modulus, E:	75 [MPa]
Shear Modulus, G:	24 [MPa]

Table 3: The Material Properties of Rohacell® 51 RIMA [10]

During the deflection of the control surface the compliant part undergoes significant amount of strains in its plane while the rigid part experiences almost zero strain, and behaves as if it was undergoing a rigid body rotation. The term "rigid part" stems from this fact.

2.2 Deflection Mechanism of the Control Surface

In order to deflect the control surface, the servo actuators are utilized and located inside the control surface volume. Volz DA-13-05-60 servo actuator [11] was found to be the smallest servo actuator to fit inside the available volume while still providing the required actuation torques. The side view of the hybrid trailing edge control surface together with the utilized servo actuators is shown in Figure 5. Figure 5 also indicates the part called the transmission part which is used to transmit the servo actuator forces to the control surface.

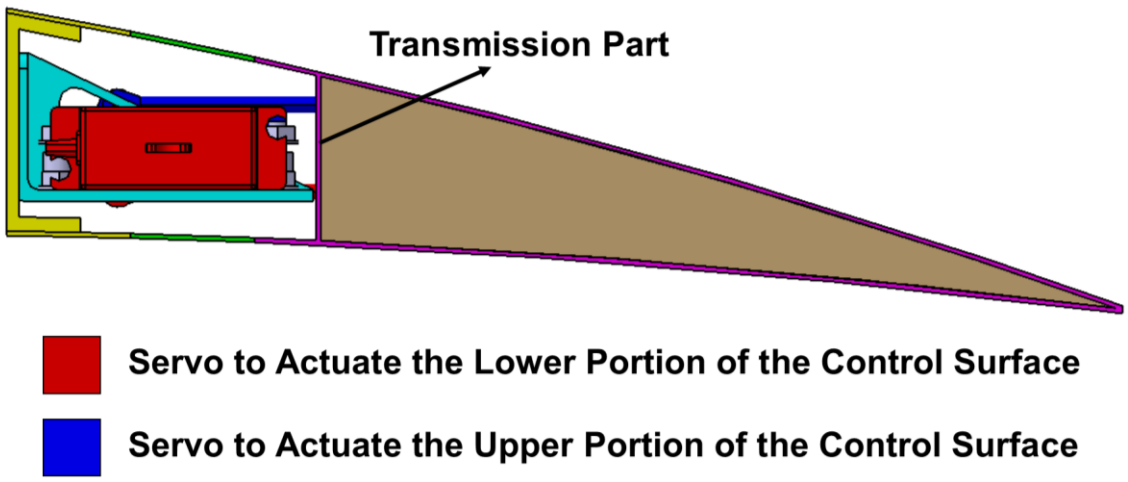

Figure 5: The Side View of the Hybrid Trailing Edge Control Surface along with the Servo Actuators

A total of five servo actuators is used in the design, that is, three servos actuate the lower portion of the control surface, and two servos actuate the upper portion of the control surface. The purposes were to estimate the upward displacement capability (*i.e.* decamber) as well as the downward displacement capability of those actuators (*i.e.* camber). The top view of the servo actuators is shown in Figure 6 along with the relevant dimensions.

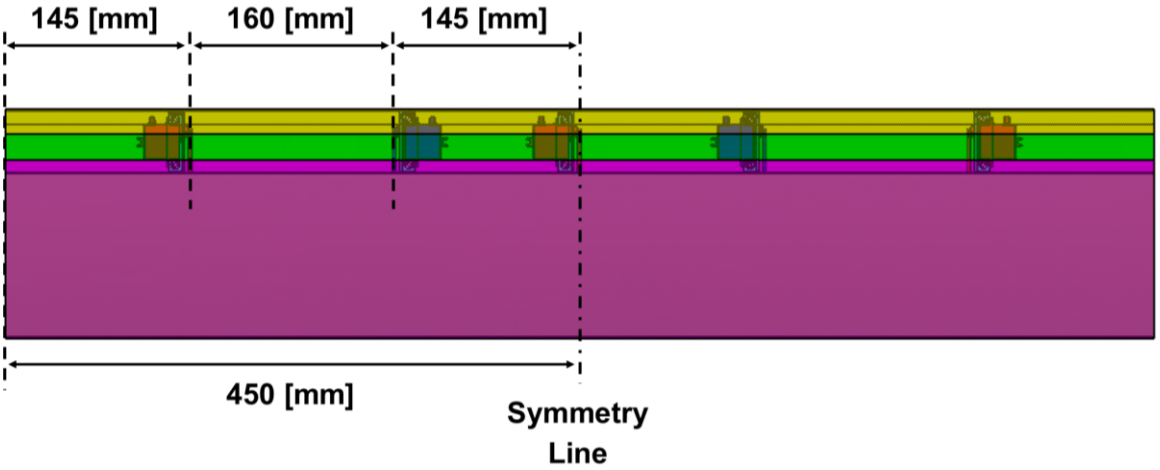

Figure 6: Top View of the Servo Actuators and the Hybrid Trailing Edge Control Surface

3 STRUCTURAL ANALYSES IN IN-VACUO CONDITION

The structural analyses were performed with Finite Element Method, using commercial software ANSYS® Workbench™ v14.0. Initially, the analyses were performed in in-vacuo condition in order to determine whether the designed control surface successfully morph into the target profiles or not and the relevant aerodynamic loads were then applied. The generated CATIA solid model of the control surface was imported to ANSYS® and the Finite Element Model was generated. In the Finite Element Model, the aluminum C part and the servo actuators themselves were not included, however, the moment arms and actuation rods of the servo actuators were modelled. The isometric view of the generated mesh of the Finite Element Model is shown in Figure 7.

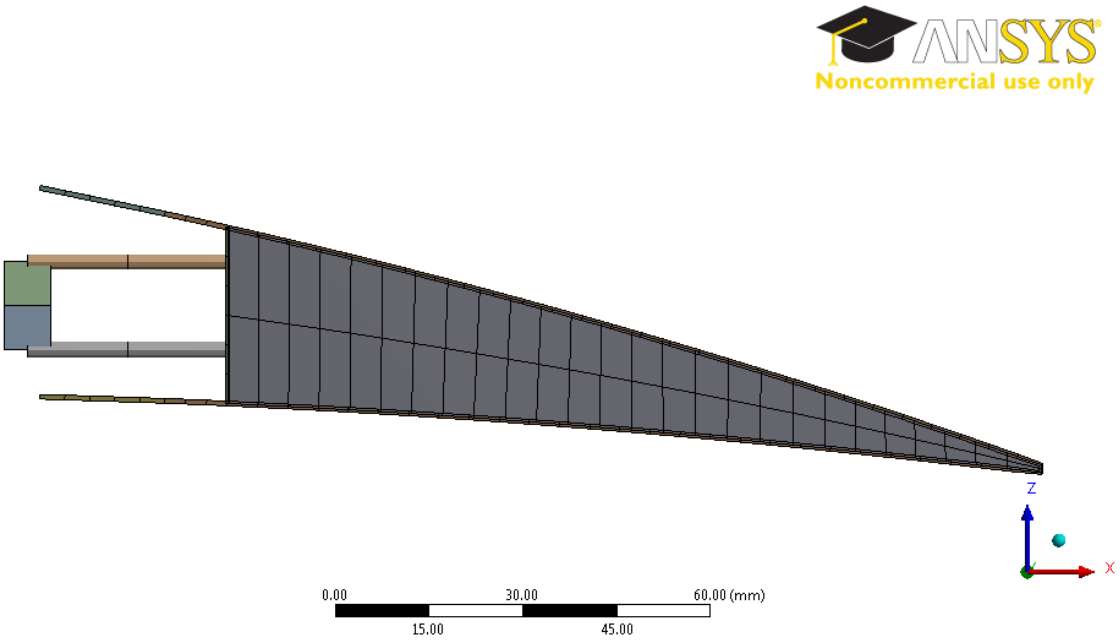

Figure 7: Isometric View of the Structural Mesh

The compliant and rigid parts were meshed with uniform quadrilateral shell elements with a thickness of 0.75 [mm]. In the rigid part, three plies were used to model the composite with ply orientation 0°/90°/0°, zero degree indicates the chordwise direction while ninety degree indicates the spanwise direction. The foam part was meshed with brick elements. The moment arms and actuation rods were modelled with beam elements. The applied boundary conditions are shown in Figure 8.

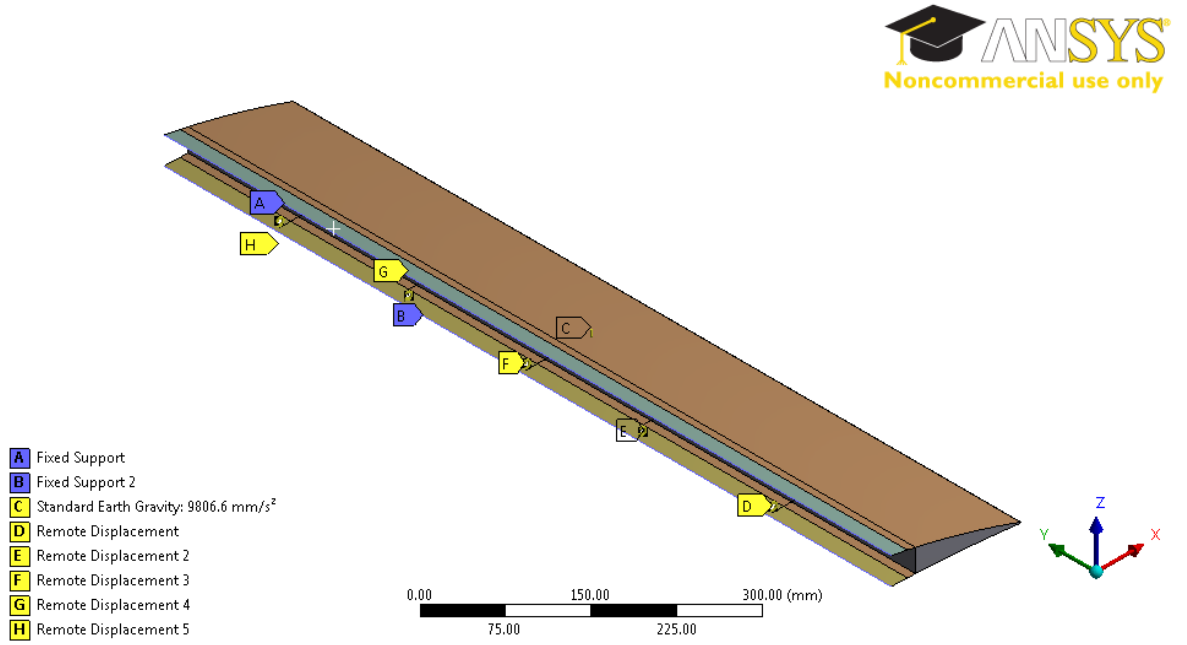

Figure 8: Applied Boundary Conditions in Finite Element Model

The parts indicated by A and B in Figure 8 were fixed in all degrees-of-freedom. The rotational boundary conditions were prescribed to the vertices of the moment arms to model the servo actuation. Additionally, gravitational load was also included to the system in order

to take into account the weight effects. The connection between the moment arms and the actuation rods are generated by pinned connection. In order to model this, the coinciding nodes of the moment arms and the actuation rods were coupled in all displacement and rotational degrees-of-freedom, except for the rotational degree-of-freedom about y axis, shown in Figure 8. The rotational boundary conditions required to achieve the target profiles are given in Table 4.

	NACA 8510	NACA 3510	NACA 2510
Servos to Actuate the Lower Portion of the Control Surface	6 [deg]	22.6 [deg]	33.4 [deg]
Servos to Actuate the Upper Portion of the Control Surface	14 [deg]	11.8 [deg]	19.1 [deg]

Table 4: The Required Rotational Boundary Conditions to Achieve the Target Profiles

The solution was performed with non-linear solver, in order to take into account the material and geometric non-linearities. The obtained transverse displacement contours (displacement in z direction) are shown in Figure 9 to Figure 11 for NACA8510, NACA 3510 and NACA 2510 respectively.

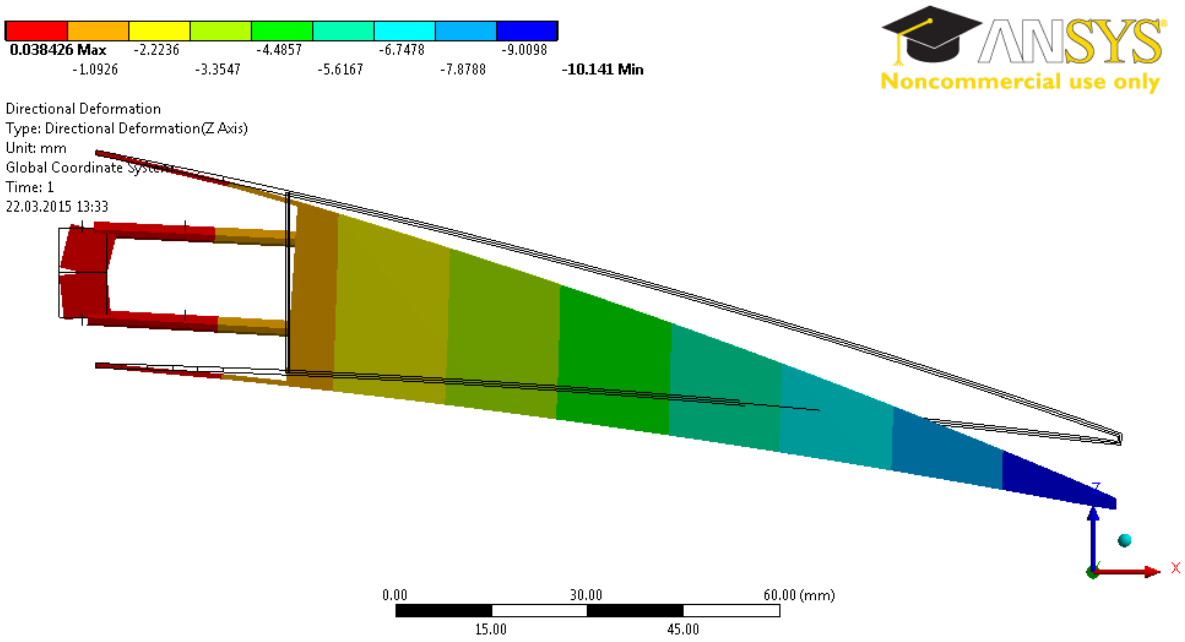

Figure 9: Transverse Displacement Contours (in z direction) for NACA 8510 Morphing in in-Vacuo Condition

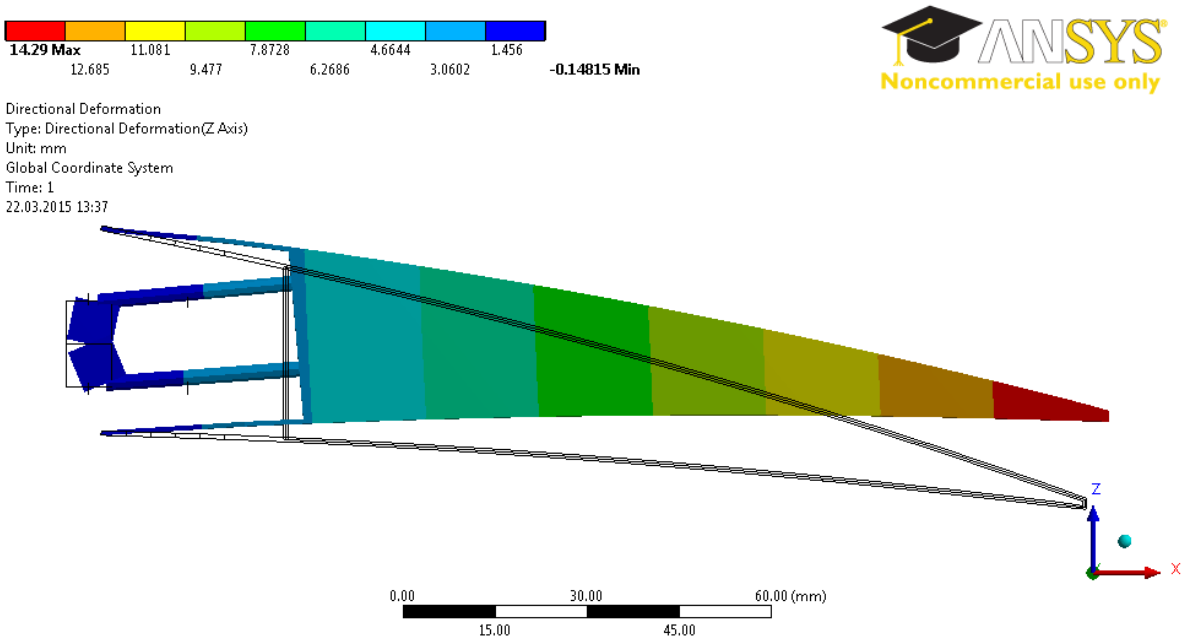

Figure 10: Transverse Displacement Contours (in z direction) for NACA 3510 Morphing in in-Vacuo Condition

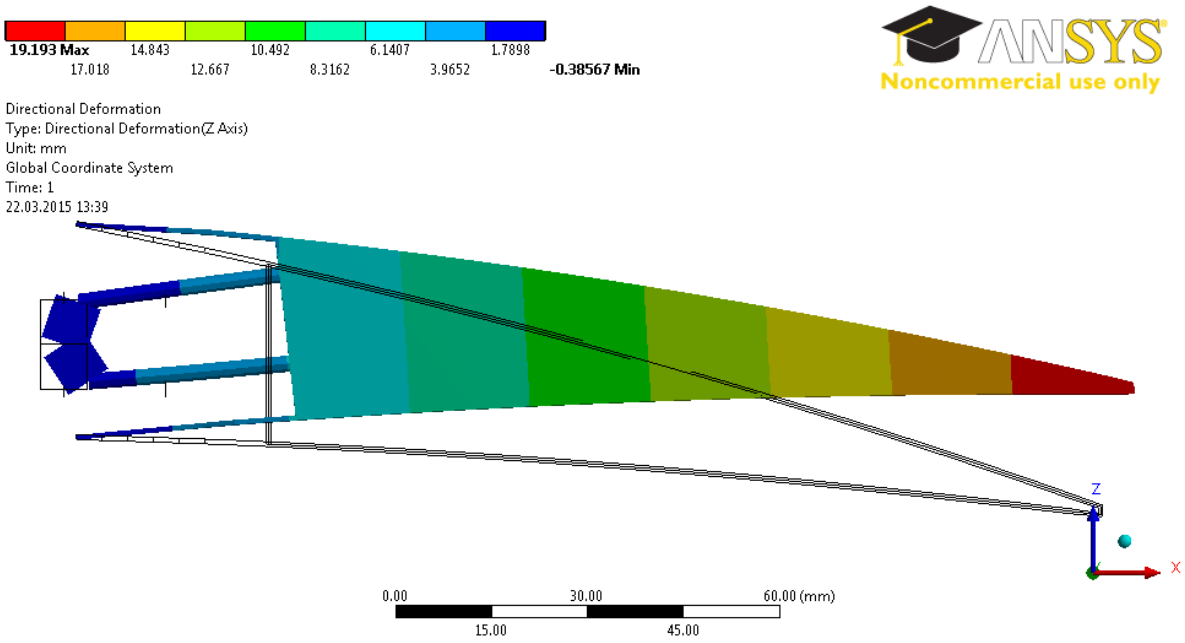

Figure 11: Transverse Displacement Contours (in z direction) for NACA 2510 Morphing in in-Vacuo Condition

Figure 12 which shows the maximum principal strain contours of NACA 2510 profile further illustrates the fact that no deformation occurs in the so-called rigid part.

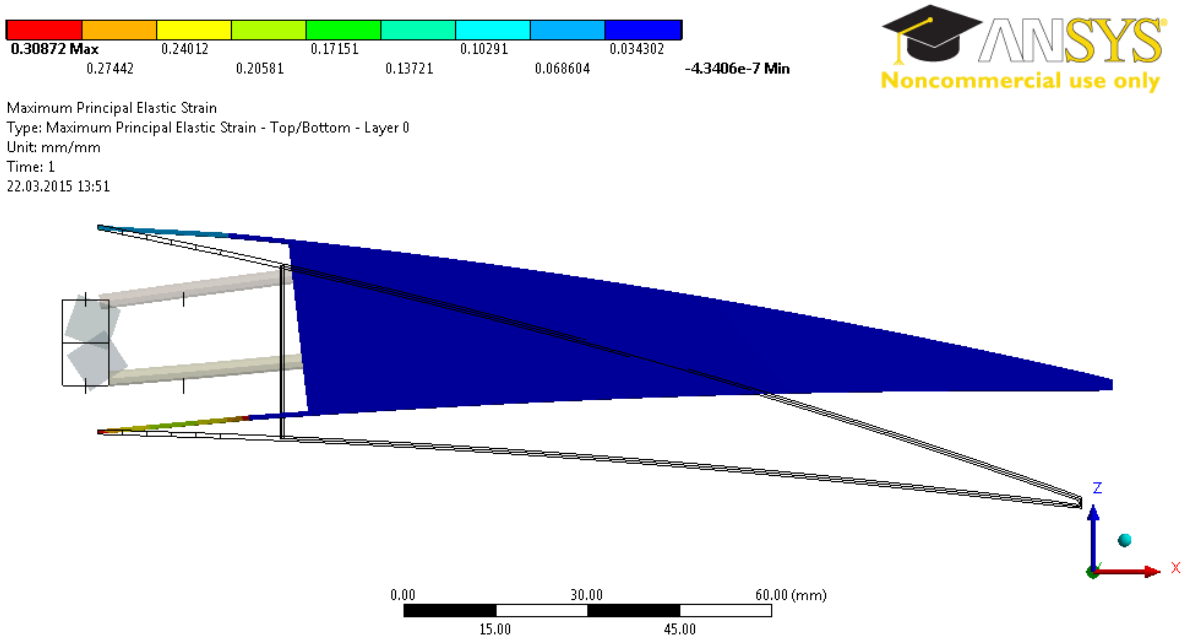

Figure 12: Maximum Principal Strain Contours for NACA 2510 Morphing in in-Vacuo Condition

As it can be seen from the Figures 9 to 11, the designed hybrid trailing edge control surface successfully morphs into target profiles in in-vacuo condition.

4 AERODYNAMIC ANALYSES

After completing the structural analyses in in-vacuo condition, aerodynamic analyses were performed to calculate the aerodynamic loads on the control surface. In aerodynamic analyses, the mesh was generated by Pointwise® V17.2 R2 package program and the solution was performed via Computational Fluid Dynamics. SU2 (Stanford University Unstructured) V3.2.1 open source software was used as solver.

The generated two dimensional surface mesh over the wing and control surface is shown in Figure 13. The generated three dimensional hemisphere outer domain is illustrated in Figure 14. Additionally, the boundary layer mesh to take into account viscous effects is given in Figure 15.

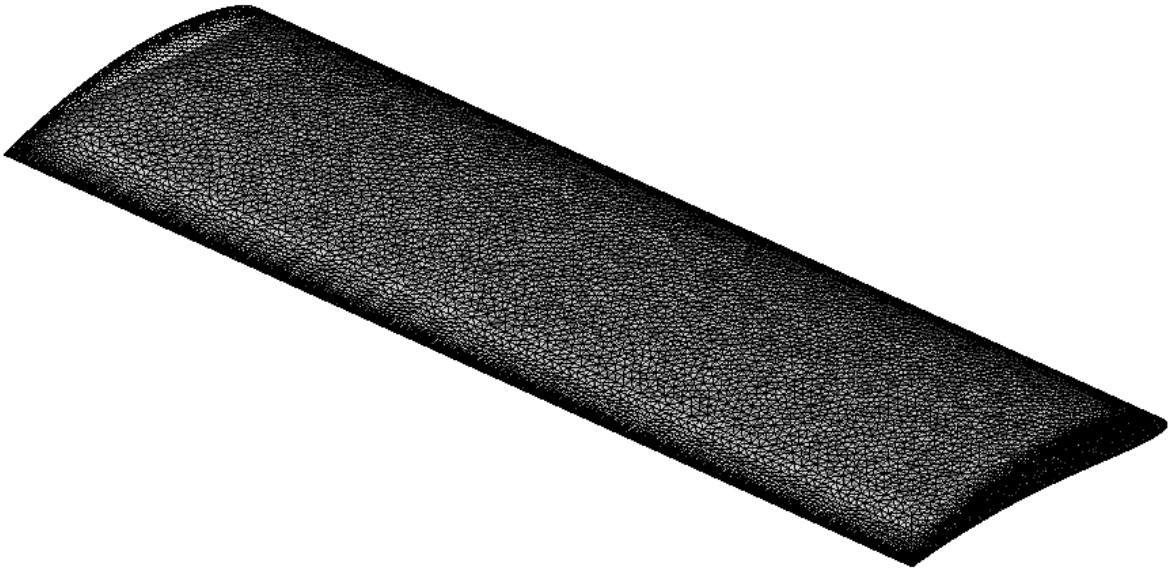

Figure 13: The Generated Two Dimensional Surface Mesh over the Wing and Control Surface

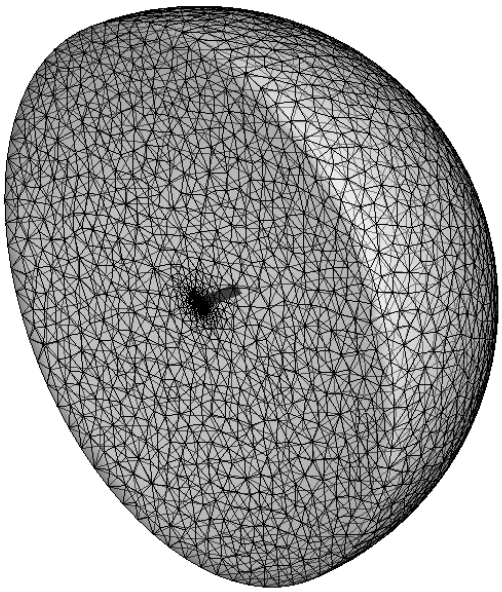

Figure 14: The Generated Three Dimensional Hemisphere Outer Domain

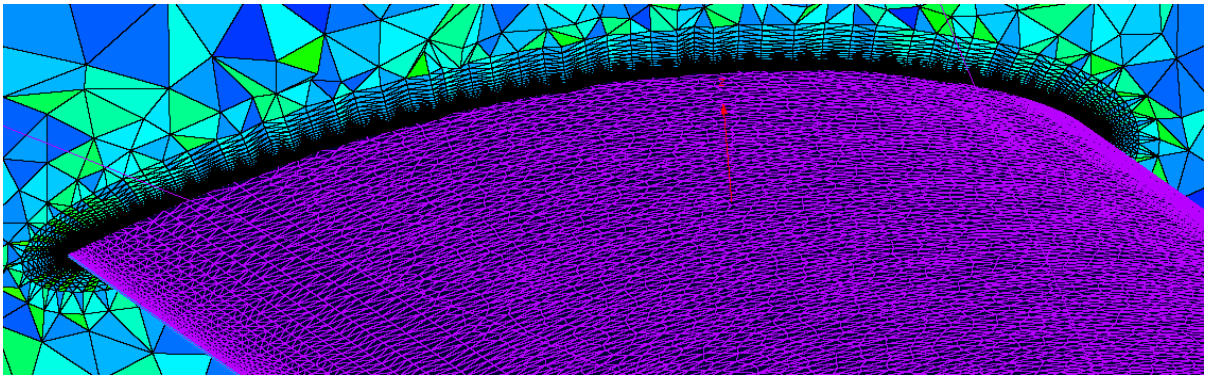

Figure 15: The Generated Boundary Layer Mesh over the Wing

The relevant flight conditions given in Table 5 were used and the solutions were performed under 1g condition. In the analyses, the flow was assumed to be viscous with Reynolds Averaged Navier-Stokes (RANS) model coupled with Spalart-Almaras turbulence modelling. Since the flight Mach numbers are relatively low, solutions were performed with incompressible model.

	NACA 8510	NACA 3510	NACA 2510
Flight Speed [m/s]	13.244	21.152	30.556
Angle of Attack [deg]	6.373	1.7131	1.056
Reynolds Number	524536	857990	1210135
Density [kg/m^3]	1.1895	1.225	1.1895
Mach Number	0.039	0.063	0.0901
Altitude [ft]	1000	0	1000

Table 5: The Input Parameters of Flight Conditions for Morphed Configurations

The calculated aerodynamic loads were transferred on to structural mesh by the property of ANSYS. The transferred pressure contours are given in Figure 16 to Figure 18 for NACA8510, NACA 3510 and NACA 2510 respectively.

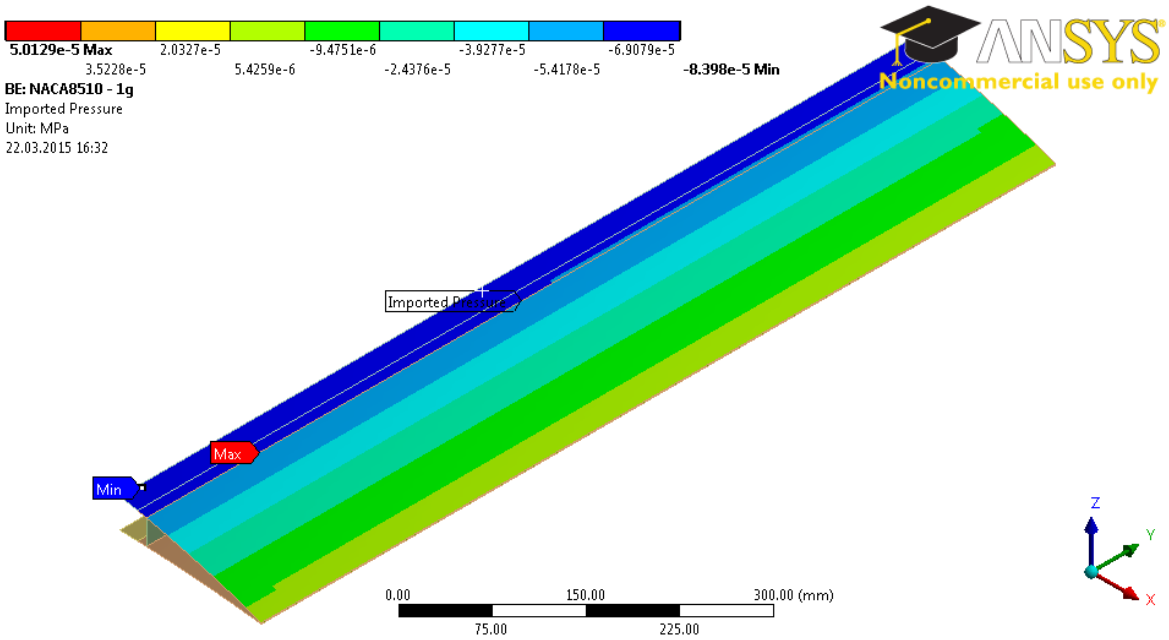

Figure 16: Imported Pressure Contours for NACA 8510 Morphing

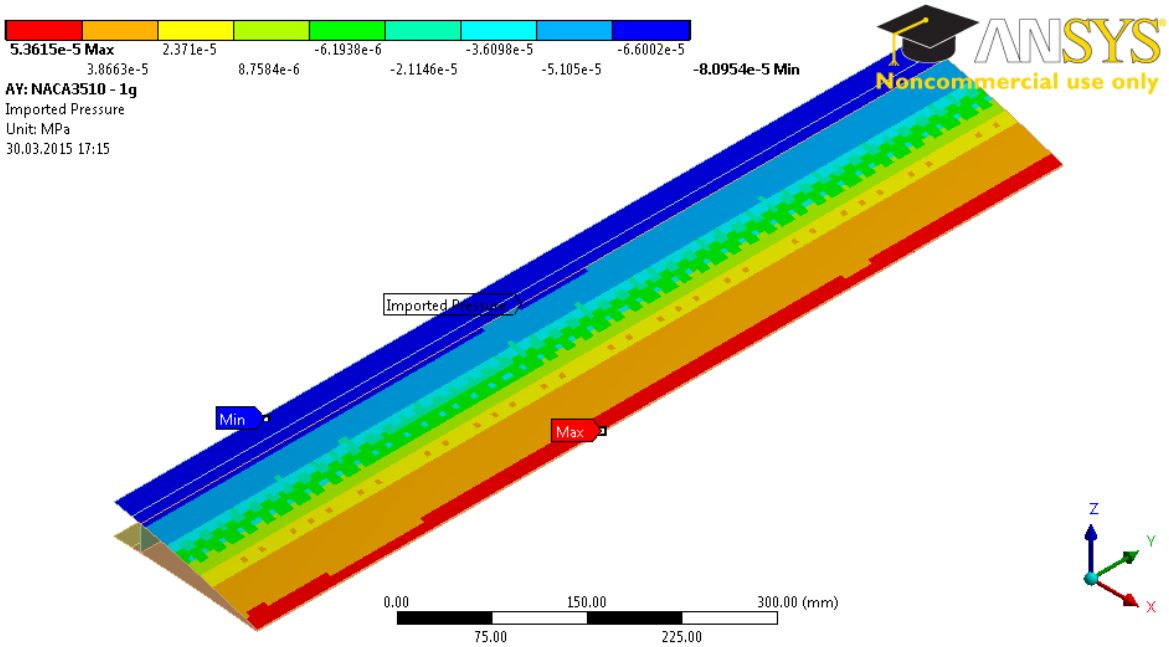

Figure 17: Imported Pressure Contours for NACA 3510 Morphing

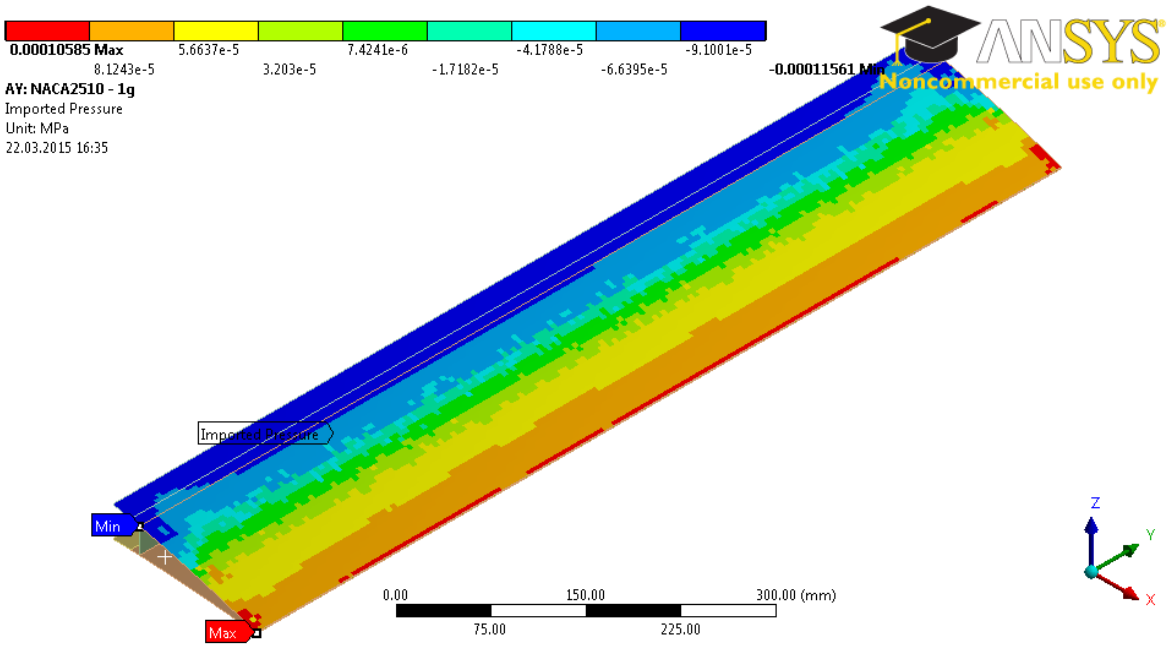

Figure 18: Imported Pressure Contours for NACA 2510 Morphing

5 STRUCTURAL ANALYSES UNDER AERODYNAMIC LOADING

After transferring the aerodynamic loads on to structural mesh, the structural analyses were conducted to assess the morphing capability of control surface under aerodynamic loading. The obtained transverse displacement (displacement in z direction) contours are shown in Figure 19 to Figure 21 for NACA8510, NACA 3510 and NACA 2510, respectively.

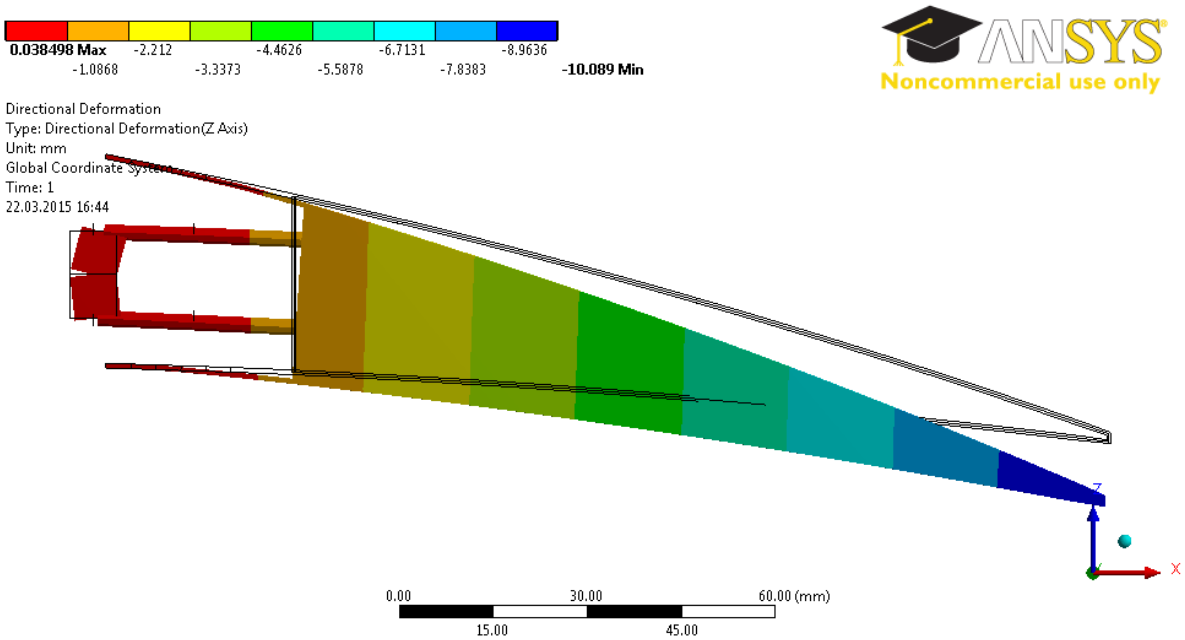

Figure 19: Transverse Displacement Contours (in z direction) for NACA 8510 Morphing under Aerodynamic Loading

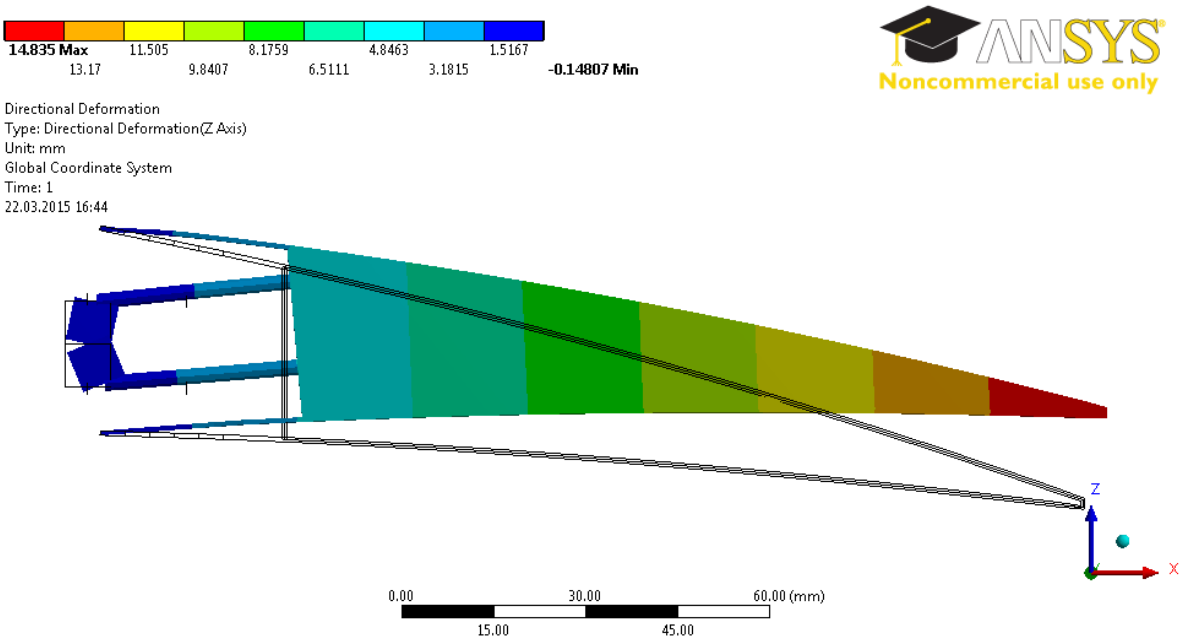

Figure 20: Transverse Displacement Contours (ln z direction) for NACA 3510 Morphing under Aerodynamic Loading

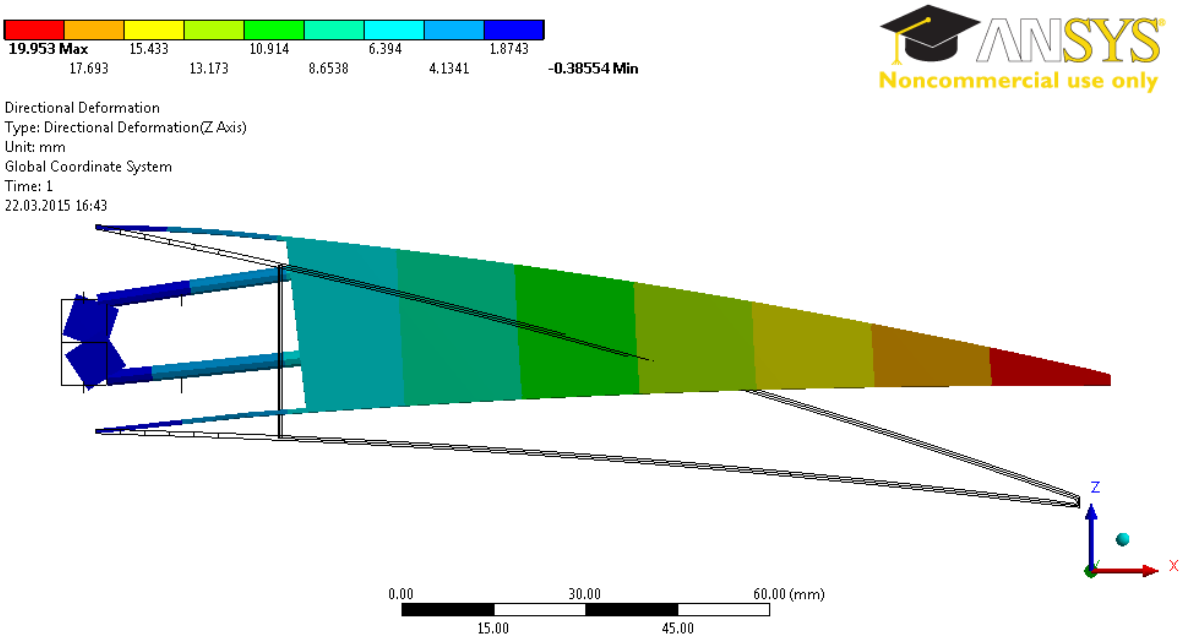

Figure 21: Transverse Dispalcement Contours (in z direction) for NACA 2510 Morphing under Aerodynamic Loading

6 CONCLUSIONS

In this study, the design and analyses of a novel hybrid trailing edge control surface are presented. It was concluded that the designed control surface can effectively perform to required camber and decamber morphing. This design will be manufactured and wind tunnel, ground vibration and flight tests will be performed.

The work presented herein has been partially funded by the European Community's Seventh Framework Programme (FP7) under the Grant Agreement 314139. The CHANGE project ("Combined morphing assessment software using flight envelope data and mission based morphing prototype wing development") is a L1 project funded under the topic AAT.2012.1.1-2 involving nine partners. The project started in August, 1, 2012.

İlhan Ozan Tunçöz and Yosheph Yang thank to TÜBİTAK (The Scientific and Technological Research Council of Turkey) for supporting them during their graduate education

REFERENCES

[1] T. A. Weisshaar. Morphing Aircraft Technology - New Shapes for Aircraft Design. In Multifunctional Structures / Integration of Sensors and Antennas, Neuilly-sur-Seine, France, 2006. Meeting Proceedings RTO-MPAVT-141

[2] M. Kintscher, M. Wiedemann, H. Monner, O. Heintze, and T. Kühn. Design of a Smart Leading Edge Device for Low Speed Wind Tunnel Tests in the European Project SADE. International Journal of Structural Integrity, 2(4):383-405, 2011

[3] P. Arslan, U. Kalkan, H. Tıraş, İ. O. Tunçöz, Y. Yang, E. Gürses, M. Şahin, S. Özgen, Y. Yaman. A Hybrid Trailing Edge Control Surface Concept. DeMEASS-VI, 6th Conference for Design, Modelling and Experiments of Advanced Structures and Systems, 25-28 May 2014, Ede-Wageningen, Netherlands

[4] P. Arslan, U. Kalkan, H. Tıraş, İ. O. Tunçöz, Y. Yang, E. Gürses, M. Şahin, S. Özgen, Y. Yaman. Structural Analysis of an Unconventional Hybrid Control Surface of a Morphing Wing. ICAST2014: 25th International Conference on Adaptive Structures and Technologies, 06-08 October 2014, The Hauge, Netherlands

[5] CHANGE FP7 Project, http://change.tekever.com/

[6] INVENT GmbH, http://www.invent-gmbh.de/

[7] ANSYS Workbench v14.0, Material Library

[8] Dow Corning 732 Silikon, http://www.swiss-composite.ch/pdf/t-Silikon-Kleber-DC-732.pdf

[9] Cambridge University Engineering Department, "Materials Data Book", 2003, pp. 10, http://www-mdp.eng.cam.ac.uk/web/library/enginfo/cueddatabooks/materials.pdf

[10] Rohacell Rima Product Information, http://www.rohacell.com/sites/dc/Downloadcenter/Evonik/Product/ROHACELL/product-information/ROHACELL%20RIMA%20Product%20Information.pdf

[11] Volz Servos, http://www.volz-servos.com/English/13mmClass/